Experiments in Fluids 34 (2003) 324–331
DOI 10.1007/s00348-002-0560-2

Details on the intermittent transition to turbulence of a locally forced plane Couette flow

G. Antar, S. Bottin, O. Dauchot, F. Daviaud, P. Manneville

Abstract Experimental results are presented on the transition to turbulence of a plane Couette flow locally and permanently forced by a small bead. The intermittent aspect of this transition is investigated in a detailed analysis of the transition periods from coherent to turbulent and vice versa. A maximum number of transitions are achieved at a Reynolds number of about 310. It is shown that the breakdown of the flow coherence results from a complex succession of events occurring as follows. A secondary instability takes place leading to a drift of at least one vortex pair away from the excitation source. Consequently, the flow in the bead vicinity is laminar and a vortex pair is generated. Turbulence results from the interaction between the newly born vortex and the one already active. As the fluctuation intensity decreases all over the flow, the laminar state is recovered in the bead vicinity from which two vortex pairs are regenerated. The second main contribution of this paper is the study of the turbulent state using spatio-temporal correlation. The role of lateral streaks and their properties in the turbulent state are investigated. It is demonstrated that the turbulent spot is sustained by a vortex generation near the source followed by convection towards the boundaries. In both coherent and turbulent states, the flow near the bead is found to determine the plane Couette flow evolution.

1 Introduction

Plane Couette flow (pCf) has received much attention mainly because of the apparent early discrepancy between theory and experiment. While, it was demonstrated that pCf is linearly stable for all Reynolds numbers (Darzin and Reid 1981), experimental investigations showed that turbulence appears at finite Reynolds numbers (*Re*) of less than 750 indicating that Couette flow is unstable for finite disturbances (Reichert 1956). Leutheusser and Chu (1971) using air with one fixed wall found a critical Reynolds number Rc=280.

The first finite-amplitude solutions of a pCf were obtained by Nagata (1990) at $Re \geq 500$. He considered the problem of a circular Couette system between co-rotating cylinders with a narrow gap. By following a series of bifurcation to the case with zero average rotation rate, he succeeded in determining steady solution in the form of co-flow modulated rolls. Later, these solutions were found unstable by Clever and Busse (1992). Recent investigations by Schmiegel and Eckhardt (1997) suggest that a chaotic repeller could underline the transition to turbulence and thus explain the unstable character of Nagata's solutions. In parallel to Nagata's work, several researchers (Butler and Farrell 1992; Farrell and Ioannou 1993; Trefethen et al. 1993; Schmid and Henningson 1992) emphasized the role of non-normality of the linear operator in the transition to turbulence. They considered the linearized Navier–Stokes incompressible equations of motion and obtained, in addition to the Orr–Sommerfeld equation, another equation describing the evolution of wall normal vorticity. Accordingly, the linear coupling between wall normal vorticity and the wall normal velocity could lead to an algebraic growth of the instability at Reynolds number much smaller than those predicted by the eigenvalue analysis. This is done by extraction of energy from the mean flow by structures such as streamwise vortices. A different approach based on extracting the mechanisms that sustain turbulence was performed by Waleffe (1995, 1996, 1998), and Hamilton et al. (1995). The model is based on a fundamental self-sustaining non-linear process consisting of an instability loop, according to which weak streamwise rolls disturb the streamwise velocity. The resultant inflections open up the possibility for three-dimensional fluctuations to develop, and the instability feeds back the energy to the original streamwise strolls. In this approach, it is the turbulent solution that is tracked instead of a fixed point as in Nagata's case. A comparison among the various models of subcritical transition to turbulence can be found in Baggett and Trefethen (1996).

On the other hand, the first numerical experiments performed by Orszag and Kells (1980) obtained a transition to turbulence at $Re \approx 1{,}000$ where the essential three-dimensional effects were included. However, in this work

Received: 28 February 2001 / Accepted: 30 September 2002
Published online: 6 December 2002

G. Antar (✉)
University of California San Diego,
Center for Energy Research,
9500 Gilman Drive, La Jolla,
CA 92093-0417, USA
E-mail: gantar@ferp.ucsd.edu

S. Bottin, O. Dauchot, F. Daviaud
Service de Physique de l'État Condensé,
Centre d'Étude de Saclay,
91191 Gif-sur-Yvette, France

P. Manneville
Laboratoire d'Hydrodynamique,
École Polytechnique,
91128 Palaiseau, France

no systematic search in the parameter space was performed so the critical Reynolds number should be considered as an upper limit value. Later, Lundbladh and Johansson (1991) performed a rather comprehensive numeric study of the pCf transition to turbulence and obtained a critical Reynolds number of about 375. They characterized the spots observed in the turbulent regime as a function of the Reynolds number. Tillmark and Alfredsson (1992) confirmed these results by triggering the transition by a high-amplitude pointwise disturbance generated by a fluid jet; they found Rc=360.

Recently, dedicated experiments on perturbed pCf have been conducted where a turbulent jet destabilized the pCf flow locally (Daviaud et al. 1992; Dauchot and Daviaud 1994). Their results on the critical Reynolds number roughly agree with those of Tillmark and Alfredsson (1992), that is $Rc\approx330$. Later, they induced a perturbation with a thin wire (Dauchot and Daviaud 1995) allowing them to reveal the existence of streamwise vortices involved in the destabilization process. With increasing Reynolds number, three regimes were identified, laminar ($Re<160$), streamwise vortices ($160<Re<340$), and turbulent ($Re>340$). They emphasized the coexistence of the stable and turbulent states describing the flow as subcritical. This description is in contrast to a supercritical situation where a continuous transition from laminar to turbulence occurs; an example of this transition is found in Rayleigh–Bénard flows (Manneville 1990). A comprehensive analysis of the perturbed pCf was performed by changing the wire diameter Re and the aspect ratio in (Bottin et al. 1998). A different perturbation later used a small bead attached to a thin wire in the streamwise direction (Bottin et al. 1997). The intermittent transition was characterized as function of Re via the turbulence fraction, the laminar periods and turbulence duration. Recently, a dedicated three-dimensional numerical experiment by Barkley and Tuckerman (1999) studied pCf perturbation by a thin ribbon with different heights. They confirmed the subcritical aspect of the transition by computing the linear instability threshold of the modified basic flow. Most of their results showed good agreement with experiment.

In this paper, the same experimental setup described in (Bottin et al. 1997) is used, that is, a pCf locally and permanently perturbed by a small bead. The motivation of using this setup is to help understanding the nature of the intermittent transition to turbulence of a locally forced pCf. The first part of this paper is dedicated to the description of the transition periods from the coherent to the turbulent state and vice versa. For this purpose, the Reynolds number is hereafter fixed at 310 where 60% of the data is turbulent so a maximum amount of transitions is present (Bottin et al. 1997). Our goal is to identify experimentally the bifurcations that lead to the intermittent transition to turbulence. This investigation can be put in the general framework of the various routes that laminar flows can take to become turbulent through different bifurcations with increasing control parameter. According to Landau, turbulent fluctuations result from infinite linear instabilities (Har 1965). Ruelle and Takens (1971), on the other hand, demonstrated that turbulence can be achieved much faster by non-linear interaction between the first few excited modes. This theory opened perspectives to a whole family of non-linear transitions to turbulence, namely by intermittency (Ott 1990). In addition, linear instabilities with non-normal contributions also describe a transition to turbulence of sheared flows (Trefethen et al. 1993). The first identified is the instability of a fixed point in the Poincarré map leading to intermittent transitions of types I, II, and III (Manneville and Pomeau 1980; Manneville 1990). Another type of intermittency is caused by "crises" where the initial state is one or several chaotic attractors that undergo changes (see Ott (1990) and references therein). Spatio-temporal intermittent transition was also identified resulting from a competition between a regular-absorbing and a chaotic metastable state Chaté and Manneville (1987).

In this paper we find that the intermittent transition results from different states. First, there is a basic state formed of two stable streamwise counter-rotating vortices – this is the streamwise vortices state identified in Dauchot and Daviaud (1995). The appearance of a perpendicular instability to the mean flow drives at least one of the vortices towards the boundary. In consequence, the flow in the vicinity of the bead is laminar and a vortex is generated. The interaction between the newly born streamwise vortex and the deviated one causes their coherence breakdown and the appearance of small-scale fluctuations. The stable state is restored when the fluctuations around the bead die away. The flow becomes laminar again before two stable streamwise counter-rotating vortices are born.

The second part of this work is the study of the turbulent state. The main finding is that the bead still continuously excites this state. The resultant fluctuations, which form the turbulent spot, result from a convection process of the fluctuations towards the boundaries. The goal here is thus to quantify these mechanisms that sustain the flow in the turbulent state using a spatio-temporal correlation technique.

2
Experimental facilities

The pCf is a simple shear flow formed by two plates moving in opposite directions. More information about the apparatus can be found in Daviaud et al. (1992) and Dauchot (1995). As illustrated in Fig. 1, x indicates the flow direction, the direction normal to the wall is y, and

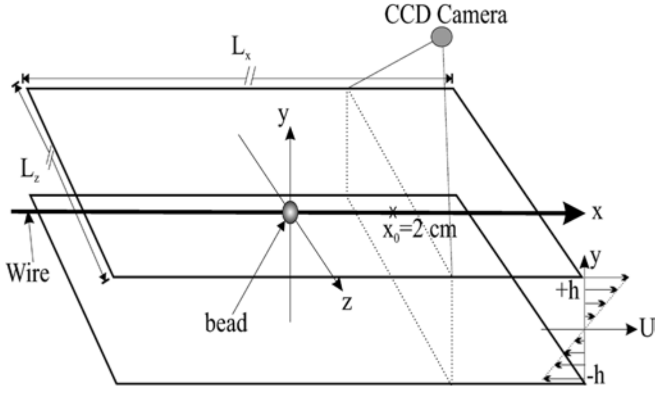

Fig. 1. Illustration of the experimental set-up

the spanwise direction is z. The bead is fixed onto the supporting wire, and its position is chosen to be the reference frame origin. The gap between the two plates is $2h$=7 mm. The sheared zone extends over an area with aspect ratios $\Gamma_x=L_x/h=285$ and $\Gamma_z=L_z/h=70$. The flow is perturbed permanently by a small sphere with radius $r/h=0.35$ placed in the central plane and attached to a thin wire, which is also in the central plane and parallel to the x direction.

The Reynolds number is defined as $Re=Uh/\nu$, where U is the speed of either walls and ν is the kinematic viscosity of water; Re in this paper is equal to 310 with an accuracy about 3%. It is chosen by consideration of the results obtained in Bottin et al. (1997) where turbulent bursts occupy about 60% of the total data string, and thus a maximum of transition periods is available.

Two types of signals are used in this paper. The spatio-temporal diagrams are obtained when water is seeded with iriodin and lit up with a 1 mm thick argon laser sheet in the (x, $y\approx0$, z) plane. From the reflected light intensity, detected by a CDD camera perpendicular to the laser sheet, the flow evolution at $x/h=5.4$ away from the bead is extracted. We denote by $\imath(z, t)$ the resultant spatio-temporal diagram, the sampling frequency being 0.2 Hz. Other information is obtained using photographs taken in the ($x\approx0$, y, z) plane after the flow is colored by yellow dye and illuminated by a laser sheet. Such photographs reflect the spatio-temporal dynamics related to vorticity at a given position to the bead.

The basic features of this perturbed pCf were discussed in Bottin et al. (1997), where it was indicated that it has similar aspects as the one produced by a thin wire or a fluid jet. The velocity profile is also similar to the one obtained with the wire perturbation where the deviation from a linear profile is observed at $|y/h|<0.2$ and at distances downstream $|x/h|<13$.

3 Intermittent transitions

When the Reynolds number is less than $R_0\approx105$, the perturbed pCf is laminar and the perturbation induced by the bead does not disturb its motion. This state is said to be "unconditionally stable", and R_0 is a global stability threshold Reynolds number (Dauchot and Manneville 1997). When $R_0 \le Re \le R_1\approx300$, pairs of counter-rotating vortices aligned in the x direction are observed. A primary supercritical instability of the system occurred leading to a three-dimensional coherent and stationary flow regime, hereafter called the coherent state.

The generated vortex pairs are symmetric and anti-symmetric with respect to the (x, y) and the (y, z) planes respectively (Bottin et al. 1997). The (y, z) photograph in Fig. 2 shows the flow circulation induced by the dissipative structure vorticity. It reveals the existence of at least two pairs of counter-rotating vortices on each side of the z axis. Their intensity, estimated as the amount of diffused light by the dragged dye, decreases with increasing distance to the bead.

Using the spatio-temporal diagrams, the positions of the two closest vortex pairs to the bead are measured each time the coherent state is recovered after a turbulent burst. The plot in Fig. 3 shows their distribution in light gray. The left- and right-hand average positions are respectively at $-4.5h$ and $+6h$ from the origin. The two distributions are thus symmetric with respect to a distance to the bead of about $z_s/h\approx+0.8$. The cause of this asymmetry with respect to the origin is still not clearly identified. However, as it will be seen later, the flow properties are symmetric with respect to this position, strongly suggesting that this asymmetry does not affect the destabilization and stabilization process. Furthermore, the asymmetry of the two counter-rotating vortices occurs in the z direction. Hence, the bead is always in the shear zone where the average velocity is zero, and the Reynolds number based on the bead is unchanged by this asymmetry.

The goal of this section is to describe in detail how the coherent state becomes unstable and how it regains its stability. By intermediate ranges, we designate lapses of time, which immediately follow or precede the turbulent bursts. The spatio-temporal diagrams used here are rather noisy because of the random presence of iriodin in the flow. In order to remedy to this problem, and so to emphasize the dynamics of the structure, a two-dimensional filter is applied

$$I(z,t) = \varphi_{a_z}(z) \times \varphi_{a_t}(t),$$

where

$$\psi_{a_t}(t) = \int \mathrm{d}t'\phi\left(\frac{t'-t}{a_t}\right)\imath(z,t') \text{ and}$$
$$\psi_{a_z}(z) = \int \mathrm{d}\zeta\phi\left(\frac{\zeta-z}{a_z}\right)\imath(\zeta,t).$$

The choice of the Gaussian function ϕ is based on the type of light fluctuations that are recorded when the flow is in the turbulent state. In the coherent state no filtering is required to emphasize the dynamics of the structure. This filter is inspired by the wavelet transform filtering technique but it does not obey the conditions $\int \mathrm{d}t\phi(t) = 0$ or $\int \mathrm{d}z\phi(z) = 0$. The parameters a_z and a_t are varied between 5 and 100 mm, and 2 to 20 s respectively. The values 10 mm ($2.9h$) and 6 s correspond to the typical scales of the fluctuations, thus, revealing best the dissipative structure properties. After filtering, a threshold is set below which the signal intensity is not plotted allowing the evolution of the structures to be emphasized. A sample of the signal is plotted in Fig. 4 where the flow is in the

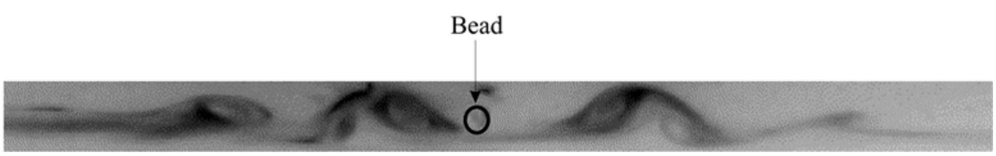

Fig. 2. A (y, z) section of the coherent state. On each side of the bead, visible at the middle of the picture, there exist at least two vortex pairs

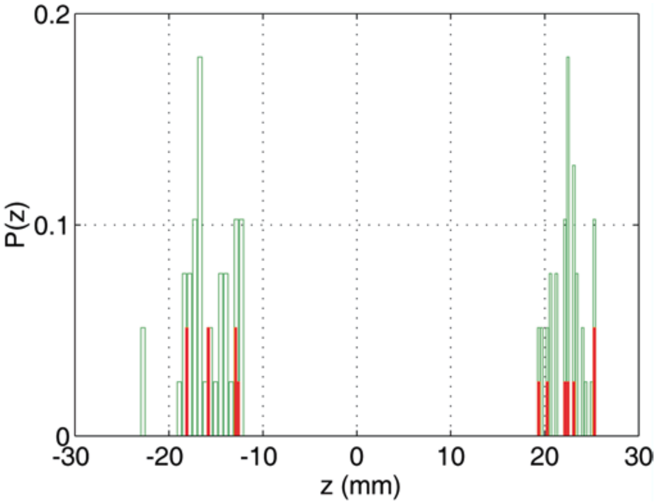

Fig. 3. The probability density of the vortex-pair positions (*gray*) and positions corresponding to the shortest durations of the coherent state between two turbulent bursts (*dark gray*)

turbulent state. In the subplot below, the filtered version is sketched. The result is more than satisfactory where the turbulent structure signal is enhanced without modifying its spatio-temporal properties.

3.1 Breakdown of the coherent state

At the Reynolds number studied here, Re=310, the flow is intermittent, staying in the coherent state for some time, then becoming turbulent and then coherent, etc. The issue of whether the positions of the vortex pairs in the coherent state is important in the breakdown process is investigated by recording the distance from the vortices to the origin that correspond to the shortest coherent periods in the intermittent signal. The distribution of such events is plotted in Fig. 3 in dark gray. The breakdown does not appear to be caused by eccentric positions of the vortex pairs in the coherent state. It is also verified that there is no statistical difference between distances to the bead before and after the turbulent bursts. Accordingly, the vortex-pair positions in the coherent state correspond to a stable state and they do not cause the intermittent flow behavior.

After investigating all of the data strings where a coherent–incoherent transition occurs, two consecutive steps were identified in the breakdown of the coherent state. In Fig. 5, two selected examples of the filtered spatio-temporal diagram are sketched.

Just before the coherence breakdown of the vortex pairs, the distance of at least one of them with respect to the origin increases. This pre-breakdown state starts up at times of about 600 and 500 s in Fig. 5a and b respectively. The vortex pair on the negative side of z drifts away from the bead before recovering a direction parallel to $\vec{x}$.

In order to verify that the drift away from the bead occurs in nearly all the transitions observed, the positions of the vortex pairs before the pre-breakdown period (denoted by $z_{+,-}$) and at its end ($z'_{+,-}$) are recorded; the indices + and – denote positive and negative sides of the z axis. In Fig. 6a, z'_{+} is plotted against z_{+}, and the solid line represents z_{+} against z_{+} in order to put forward the deviation position. In Fig. 6b, the same thing is shown for negative z. On both sides, the vortex pairs in general deviate from the coherent state values. The drift away from the bead displayed in Fig. 5 is thus statistically confirmed. Moreover, the few points indicating a shift towards the bead are caused by situations where the vortex pairs on both sides of the bead drift in the same direction. In this case, the left-hand vortex (say) records a shift towards the wall where the right-hand one produces the opposite behavior.

At this stage of evolution, two possibilities can occur: either the vortex pairs break down leading to turbulence (Fig. 6a), or they return to their initial position (Fig. 6b). The second case is particularly interesting because it

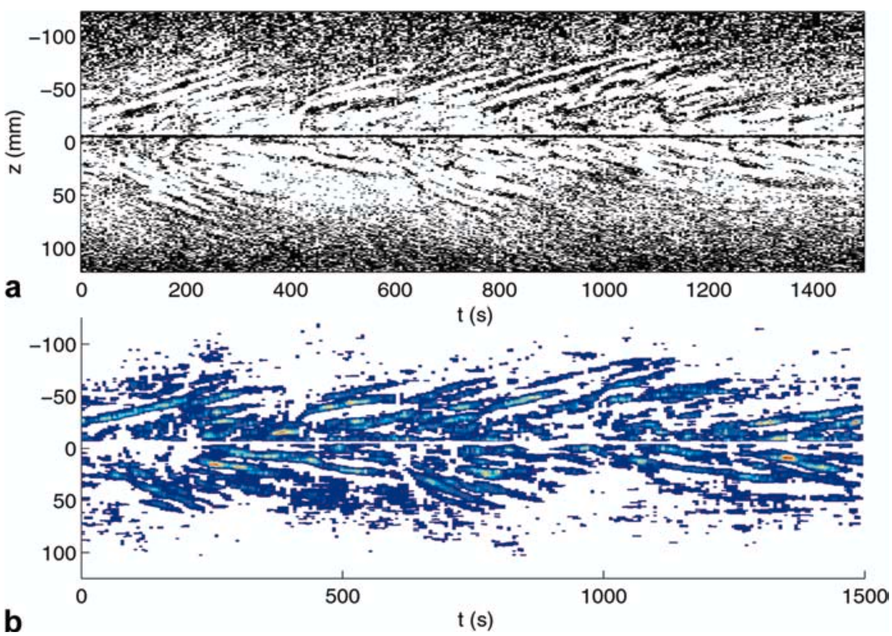

Fig. 4. A sample of the spatio-temporal diagram showing the locally forced pCf in the turbulent state (*top*), the filtered spatio-temporal diagram (*bottom*)

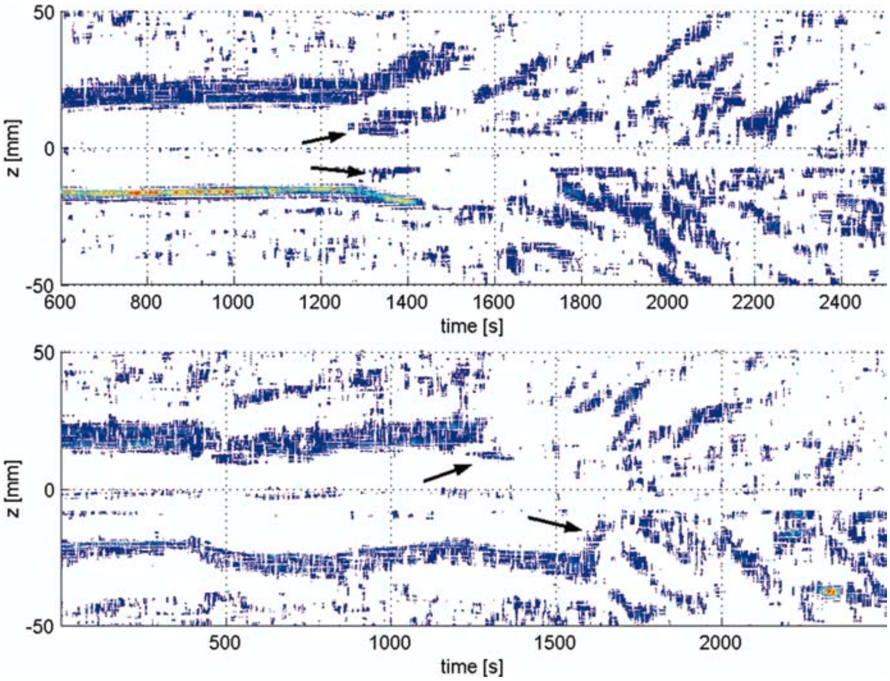

Fig. 5. Two samples of the filtered spatio-temporal diagrams showing a transition from the coherent to the turbulent state. The *arrows* indicate the newborn vortices

enables us to have a clearer image of the nature of the instability. The deviated vortex pair goes back to its initial position and drifts away again revealing an oscillation in the (x, z) plane caused by a secondary instability. When a vortex pair is relatively far from the bead, the flow in the vicinity of the latter becomes laminar and thus a primary instability is excited, generating a new vortex. In Fig. 5a and b, the newly born vortices are indicated with arrows. This new state is very unstable and breaks down to turbulence because of the interaction between the vortices created on the same side of z. Going back to the first case illustrated in Fig. 6a, the same process occurs, but the new vortex is generated in the first drift away from the bead, i.e. at half the oscillation period.

Accordingly, the transition to turbulence of the locally forced pCf occurs after several bifurcations. The state of the flow as a whole depends critically on what happens in the bead vicinity.

3.2
Collapse of the turbulence state

Figure 7 represents a typical example of when the coherent state is re-established after a turbulent burst. We point out two consecutive stages: the decay of turbulence followed by the generation of the vortex pairs. In most of the cases, turbulence decays gradually all over the space. A sudden collapse of the fluctuations is seldom observed. This fact leads to a laminar state close to the bead. Consequently, two coherent vortex pairs at $+z$ and $-z$ are generated. The latter are formed close to the bead and they appear symmetric with respect to $z\approx 0$. Then they drift away and gradually the vorticity direction tends to be parallel to $\vec{x}$.

Accordingly, the generation of the coherent state usually takes place at the same time on both sides of the bead after passing the laminar state.

4
Inside a turbulent burst

In this section, we investigate the properties of the turbulent state using spatio-temporal correlation coefficients. Having a permanent perturbation allows us to investigate

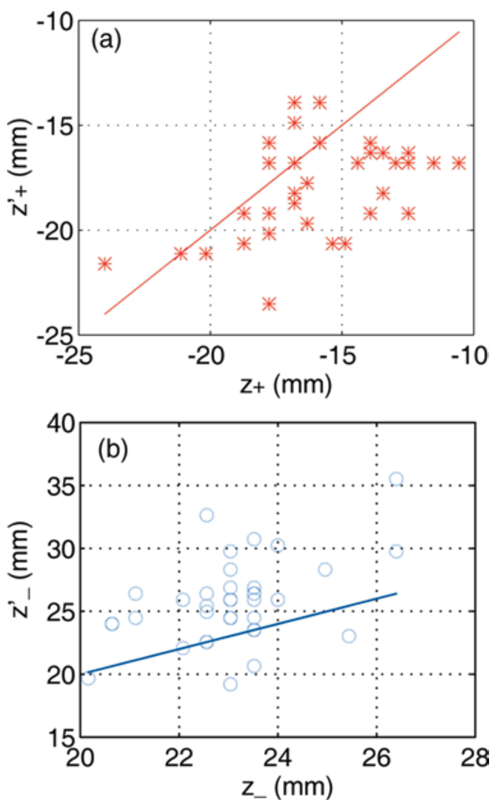

Fig. 6a, b. Positions before the pre-destabilization period (z) and at its end (z') in **a** for the positive side, and in **b** for the negative one; the straight line illustrates z vs z

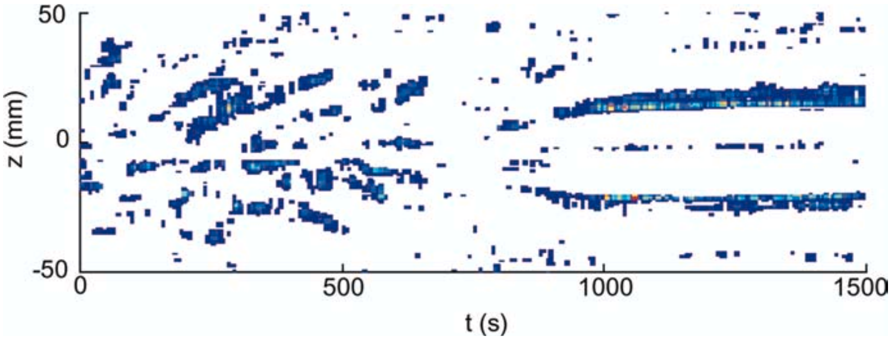

Fig. 7. The transition from a turbulent state to a coherent state; note that before the two counter-rotating vortices are born in the vicinity of the bead, the fluctuations have disappeared

the dynamics of turbulent fluctuations, which were too fast to be observed when using an instantaneous perturbation. The goal here is thus to understand the way turbulence is sustained for relatively long periods of times at such a low Reynolds number (Re=310).

Looking at Fig. 4b, it appears that turbulence is sustained by either a continuous generation of vortex pairs near the bead followed by a drift away from it, or by a generation at a given time of a certain number of periodic structures with wavelength increasing in time (the coherent part of the turbulent fluctuations is called streaks). The interaction among the vortices generates a random-like motion.

The statistical properties of turbulence are characterized by the spatio-temporal correlation coefficient defined as

$$C(z_0, \mathrm{d}z, \tau) = \frac{\langle I_{z_0}(t) I_{z_0+\mathrm{d}z}(t+\tau)\rangle}{\sqrt{\langle I_{z_0}(t)^2\rangle\langle I_{z_0+\mathrm{d}z}(t)^2\rangle}},$$

where z_0 and dz denote respectively a position and a width. Spatial characteristics are obtained by changing dz and keeping z_0 constant $(C_{z_0}(z = z_0 + \mathrm{d}z, \tau))$, or vice versa ($C_{\mathrm{d}z}(z_0,\tau)$), whereas temporal dependence is obtained by varying τ. In this section, a data string where the flow is turbulent over T=15,000 s is used.

4.1
The spatio-temporal correlation at fixed z_0

The relation between $I(z_0, t)$ and its surrounding, $I(z=z_0+\mathrm{d}z, t+\tau)$ is quantified by $C_{z_0}(z, \tau)$ where z_0 takes some chosen values, and dz and τ are varied.

Figure 8 illustrates the spatio-temporal correlation for z_0=2, 10, 20, and 30 mm (0.6, 2.9, 5.7, and 8.6h). The colors represent the correlation amplitude changing linearly from dark blue to violet.

At z_0=2, the spatio-temporal correlation width in time and space is small indicating that perturbations at such distances from the origin are not yet coherent in the sense of long-lived dissipative structures. This aspect dramatically changes as z_0 is increased, when a high-amplitude correlation is recorded over an oblique large area reflecting auto-correlation of the vortices moving in the (z, t) space. Furthermore, the correlation among the parallel vortices is reflected in parallel oblique structures observed in the last right-hand subplot in Fig. 8. The distance between the parallel correlation fingers yields a wavelength $\lambda\approx$20 mm (5.7h). One can also deduce the average scale of the dissipative structures from the spatio-temporal correlation half-width, and their velocity is estimated from the slope that the correlation amplitude makes in the (z, t) space. These properties appear in Table 1 for the different values of z_0.

4.2
The spatio-temporal correlation at fixed dz

In this subsection, z_0 is changed between 0 and 50 mm (0 to 14.3h), and dz is fixed. The color mapping is the same as in the previous section depending on the amplitude of $C_{\mathrm{d}z}(z_0, \tau)$. For d$z$=1 mm (0.3$h$), the first left-hand plot in Fig. 9 indicates high correlation with maximum values of about $\tau_0\approx$0. The amplitude decreases as z_0 tends to the boundaries indicating that these areas are less visited. This fact is clearer in the next figure, where dz=5 mm (1.4h) and maximum correlation is attained at $\tau_0\approx$20 s. This reflects an average delay time between fluctuations separated by a distance of 1.4h caused by the oblique propagation of the vortices. When the distance between the two correlated

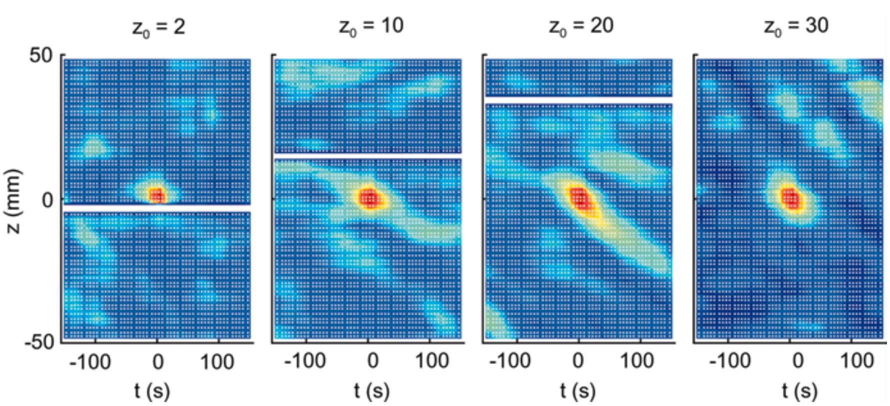

Fig. 8. The spatio-temporal correlation determined for four positions of z_0. The horizontal white line in each subplot schematizes the wire position

Table 1. Properties of structures in the turbulent state

z_0 (mm)	2 (0.57h)	10 (2.86h)	20 (5.71h)	30 (8.57h)
Average velocity (mm/s)	0	0.1	0.23	0.28
Average length (mm)	8.7 (2.5h)	21.7 (6.2h)	43.4 (12.4h)	22 (6.3h)

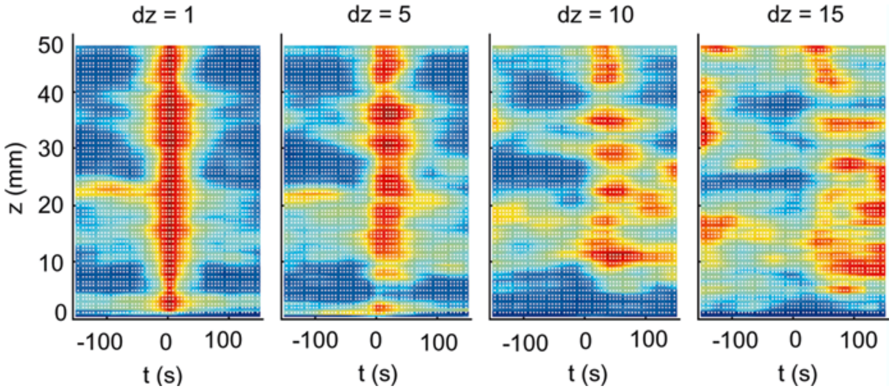

Fig. 9. The spatio-temporal correlation determined for four values of dz

signals is multiplied by a factor of two, dz=10 mm (2.9h), the average delay time becomes $\tau_0 \approx 40$ s. At dz=15 mm (4.3h) a non-negligible correlation amplitude is recorded about $\tau_0 \approx 100$ s.

The overall correlation amplitude decreases with increasing dz reflecting the long time and distance incoherence of the structures. We also note the decrease of the correlation amplitude in the vicinity of the bead ($z_0/h \leq 2.3$), which is in agreement with the results of the previous section.

Accordingly, we deduce that turbulence is generally formed from parallel oblique vortices. They are born in the vicinity of the bead, they live and gain coherence at distances about 20 mm (5.7h) from it, and they die when $z \approx 60$ mm (17h) is exceeded. Therefore, even in the turbulent state, the pCf dynamics is determined by what is happening in the bead vicinity. Even though the turbulent spot extends over a large region in space, it is still sustained by the local source. The space filling is accomplished by a convective process that drives the vortices toward the boundaries.

5
Conclusion

A detailed investigation of the locally forced pCf is carried out at a Reynolds number equal to 310. The existence of a state, which precedes the generation of turbulence, is identified. In this state, the vortices remain coherent but subject to oscillations in the (x, z) plane (perpendicular to the coherent state vortex directions), which leads to a drift of the vortices towards the boundaries. The period of such oscillation is estimated at about 800 s. Consequently, the state of the flow in the bead vicinity becomes laminar, which excites the primary instability leading to the generation of a new vortex. The interaction between this new vortex and the one already there breaks their coherence and leads to turbulence. However, the 800 s period is not often observed because a new vortex is generated after the first drift at half the oscillation period. The return to the coherent state is generally the result of the collapse of the fluctuations all over the sheared region. The flow being laminar again, it is re-excited by the primary instability leading to the coherent state.

In the turbulent state, the distance to the origin is found to play an important role in the generation of turbulence and its spatial extension. This fact was demonstrated using the spatio-temporal correlation coefficient that clearly reflected the oblique motion in the (z, x) space. We are able to assess some of the incoherent vortices properties such as their average velocity, the distance above which they gain coherence, their lifetime and the average distance between them. Most important, we showed that vortices are born in the bead vicinity and they are convected away. When they reach distances where the initial kinetic energy cannot overcome dissipation, they vanish.

References

Baggett JS, Trefethen LN (1996) Low-dimensional models of subcritical transition to turbulence. Phys Fluids 9:1043–1053
Barkley D, Tuckerman LS (1999) Stability analysis of perturbed plane Couette flow. Phys Fluids 11:1187–1195
Bottin FDS, Dauchot O, Daviaud F (1997) Intermittency in a locally forced plane Couette flow. Phys Rev Lett 79:4377–4381
Bottin FDS, Dauchot O, Daviaud F, Manneville P (1998) Phys Fluids 10:2597–2607
Butler KM, Farrell BF (1992) Three-dimensional optimal perturbations in viscous shear flow. Phys Fluids A 4:1637–1650
Chaté H, Manneville P (1987) Transition to turbulence via spatio-temporal intermittency. Phys Rev Lett 58:112–116
Clever RM, Busse FH (1992) Three-dimensional convection in a horizontal fluid layer subjected to a constant shear. J Fluid Mech 234:511–526
Darzin PG, Reid WH (1981) Hydrodynamic stability. Cambridge University Press, Cambridge
Dauchot O (1995) Transition sous-critique vers la turbulence. Cas de l'écoulement de Couette plan. Thesis, Université Paris VI
Dauchot O, Daviaud F (1994) Finite amplitude perturbation and spot growth mechanism in plane Couette flow. Phys Fluids 7:335–343
Dauchot O, Daviaud F (1995) Streamwise vortices in plane Couette flow. Phys Fluids 7:901–903
Dauchot O, Manneville P (1997) Local versus global concepts in hydrodynamic stability theory. J Phys II 7:371–389
Daviaud HF, Hegseth J, Bergé P (1992) Subcritical transition to turbulence in plane Couette flow. Phys Rev Lett 69:2511–2515

Farrell BF, Ioannou PJ (1993) Stochastic forcing of the linearized Navier–Stokes equations. Phys Fluids A 5:2600–2609
Hamilton JM, Kim J, Waleffe F (1995) Regeneration mechanisms of near-wall turbulence structures. J Fluid Mech 287:317–348
Har DT (1965) Collected papers of L.D. Landau. Pergamon Press, Oxford
Leutheusser HJ, Chu VH (1971) Experiments on plane Couette flow. J Hydraul Eng Div ASCE 97:1269
Lundbladh A, Johansson AV (1991) Direct simulation of turbulent spots in plane Couette flow. J Fluid Mech 229:499–516
Manneville P (1990) Dissipative structures in weak turbulence. Academic Press, Boston, Mass.
Manneville P, Pomeau Y (1980) Different way to turbulence in dissipative dynamical systems. Physica D 1:219–226
Nagata M (1990) Three-dimensional finite-amplitude solutions in plane Couette flow: bifurcation from infinity. J Fluid Mech 217:519–527
Orszag SA, Kells LC (1980) Transition to turbulence in plane Poiseuille and plane Couette flow. J Fluid Mech 96:159–205
Ott E (1990) Chaos in dynamical systems. Cambridge University Press, Cambridge
Reichert H (1956) Über die Geschwindigkeitverteilung in einer geradlinigen turbulenten Couettesströmung. Z angew Math Mech 36:26–32
Ruelle D, Takens F (1971) On the nature of turbelence. Comm Math Phys 20:167–172
Schmid PJ, Henningson DS (1992) A new mechanism for rapid transition involving a pair of oblique waves. Phys Fluids A 4:1986–1989
Schmiegel A, Eckhardt B (1997) Fractal stability in plane Couette flow. Phys Rev Lett 79:5250–5254
Tillmark N, Alfredsson PH (1992) Experiments on transition in plane Couette flow. J Fluid Mech 235:89–102
Trefethen LN, Trefethen AE, Reddy SC, Driscoll TA (1993) Hydrodynamic stability without eigenvalues. Science 261:578–583
Waleffe F (1995) Transitions in shear flow. Nonlinear normality versus linear non-normal linearity. Phys Fluids 7:3060–3066
Waleffe F (1996) On a self-sustaining process in shear flows. Phys Fluids 9:883–900
Waleffe F (1998) Three-dimensional coherent states in plane shear flows. Phys Rev Lett 61:4140–4144